

Systematic comparison of initial velocities for neutron stars in different models

Ali Taani

Applied Science Department, Aqaba University College, Aqaba, Al-Balqa' Applied University, P.O. Box 1199, 77110 Salt, Jordan

Department of Applied Physics and Astronomy, University of Sharjah, P.O. Box 27272 Sharjah, United Arab Emirates; ali82taani@gmail.com

Received 2015 June 19; accepted 2016 March 10

Abstract I have studied the initial velocity (Maxwellian and exponential distributions) and the scale height of isolated old (aged $\geq 10^9$ yr) neutron stars (NSs) at different Galactocentric distances R in three population models. The smooth time-independent 3-D axisymmetric gravitational potentials (Miyamoto-Nagai and Paczyński models) were also used. The correlation between these quantities significantly affects the shapes of the profiles and distributions of the simulated sample, because the differences in the initial kick can arise from differences in the formation and evolution of NSs with other physical parameters. The scale height of the density distribution increases systematically with R . I have also shown that the distribution of old NSs in these population models agrees with the observed structure of the Galaxy in terms of initial velocities (1-D and 3-D), as well as the scale height distributions. These distributions tend to have an asymptotic behavior at the point $R = 2.75$ kpc. This means that the quality of the models can be described in terms of a mean of the fitted Gaussian, and this could also give an overall perspective of the phase space properties of nearby old NSs on a given gravitational potential.

Key words: pulsar: general — stars: neutron — stars: statistics — stars: evolution — Galaxy: structure — Galaxy: disk — galaxies: kinematics and dynamics

1 INTRODUCTION

Neutron stars (NSs) are believed to acquire their large initial random velocities from supernova explosions and they also arise in many cases from binary orbital motion that is disrupted by the explosions, in addition to the strongly asymmetric explosions of their progenitors, for which there is already ample observational evidence of core collapse (for recent studies and reviews of the evolution of massive stars and the mechanisms of core collapse supernovae, I refer the reader to e.g. Shklovskii 1970; Cordes et al. 1993; Spruit & Phinney 1998; Podsiadlowski et al. 2005; Lorimer 2008; Wongwathanarat et al. 2010; Taani et al. 2012a,b; Janka 2012; Wongwathanarat et al. 2015). However, the origin of their high velocities is still unclear (Han 2008; Wang & Han 2010). The physical causes and the various mechanisms for the high velocities in pulsars have been summarized by Lai et al. (2001).

The statistics of pulsar velocities have been reviewed by Hobbs et al. (2004, 2005) with the observed average of $\sim 200\text{--}500$ km s $^{-1}$, while faster cases of about 1600 km s $^{-1}$ have been observed in the Guitar Nebula (B2224+65) (Chatterjee & Cordes 2004). It is worth mentioning that estimations of pulsar velocities depend on direct distance measurements, which can be performed by

the dispersion measure-derived distance and a Galactic electron density model, and from parallax measurements (e.g. Taylor & Cordes 1993; Brisken et al. 2002).

To investigate the isolated old NS population whose characteristic age is $\tau_c \geq 10^9$ yr in the Galaxy (excluding millisecond and binary pulsars and those in globular clusters), numerical simulations have been made by a few authors with various methods (e.g. Paczynski 1990; Sun & Han 2004; Wei et al. 2005; Gonthier et al. 2006; Hu et al. 2006; Taani et al. 2012b; Taani & Vallejo 2016, submitted). In general, isolated NSs may be detected due to accretion from the interstellar medium in the case of old NSs that emit in X-ray or due to the energy released by the cooling of young NSs (see e.g. Chieregato et al. 2005 for an overview and references). This statement explains the two methods to observe the isolated NSs through (1) the X-ray emission in the old population or (2) by the cooling of young isolated NSs. Several candidates have been found by the *ROSAT* satellite through X-ray thermal radiation. This theoretical and observational progress was reviewed by many authors (see for example Tsuruta 1998; Popov et al. 2000; Yakovlev & Pethick 2004; Page et al. 2004). Masses of NSs have only been measured in a few dozen cases and their mass functions have been estimated (e.g. Zhang et al. 2011 and references therein).

Cordes & Chernoff (1998) developed a model with two Maxwellian components in kick speed having one-dimensional (1-D) velocity dispersions of $\sigma_{v1} \sim 175 \text{ km s}^{-1}$ and $\sigma_{v2} \sim 700 \text{ km s}^{-1}$. However, Hobbs et al. (2005) argued that the initial velocity distribution can be well described by a Maxwellian distribution with $\sigma_v = 256 \text{ km s}^{-1}$, which was adopted by Gonthier et al. (2007) in their simulation. In addition, Faucher-Giguère & Kaspi (2006) put forward another model in which the absolute 1-D velocity components are exponentially distributed with a three-dimensional (3-D) mean velocity of about 380 km s^{-1} .

In this paper, through analyzing the details of NS spatial distributions and velocities in the Galaxy, I study the steady state distribution of some fraction of old NSs. I considered three models of the distributions of birth velocity, Arzoumanian et al. (2002), Hobbs et al. (2005) and Faucher-Giguère & Kaspi (2006) (hereafter called Model *A*, Model *B* and Model *C*, respectively) in the 3-D axisymmetric gravitational potential adopted by Paczynski (1990) (hereafter P90) to represent a non-rotating Galactic disk. This is suitable for the simplified analysis that I develop here. I also study the NS scale heights at different Galactocentric distances R .

2 SIMULATION DETAILS

In this paper, I use the same simulated old NSs as described in Taani et al. (2012b) and the reader is referred to that paper for details. Briefly, I choose random distributions for the birthplaces, initial kick velocities and scale heights for newly born NSs. The stars were assumed to be born in the Galactic plane ($z = 0$) with circular velocities plus additional isotropic kick velocities. The distance from the Sun to the center of the Galaxy is given by $R_\odot = 8.5 \text{ kpc}$. I use the Monte Carlo method to pick an NS from these distributions and to assign an age to it, plus its kinematics is governed by the motion equations described by the P90 gravitational potential. Based on these initial conditions and the motion equation, the procedure is repeated until I have a large enough simulated sample in order to present the evolutions of NS locations and velocities, through long-term dynamics. The number of pulsar samples in the simulation is set as 1×10^7 .

2.1 Components of the Gravitational Potential

I will now combine three of the axisymmetric potential-density forms to produce a model of the matter distribution and its gravitational potential in the Milky Way. The basic components of the Milky Way are the visible Φ_{disk} and Φ_{sph} and the invisible dark matter Φ_{halo} . For the bulge (spheroid) I adopt a Plummer sphere (Plummer 1911) in order to increase the central mass of the Galaxy. For the disk, I adopt the Miyamoto-Nagai potential (Miyamoto & Nagai 1975) which is added in order to reproduce the scale length of the disk. For the dark matter halo, I adopt a logarithmic (modified sphere) potential, which produces a flat

Table 1 Initial Parameters for the Components of Galactic Potential

	a	b	Mass	q_a	q_b
Spheroid	0	0.28	1.12×10^{10}	–	–
Disk	3.7	0.2	8.01×10^{10}	1.2	0.9
Halo	–	–	8.01×10^{10}	–	–

rotation curve at large radius (Flynn et al. 1990; Binney & Tremaine 2008). These components are parametrized to match observations (see P90 for details).

The spheroidal potential and Miyamoto-Nagai potential (Miyamoto & Nagai 1975) have the advantage that their potential can be calculated analytically. Thus, they can be described as

$$\Phi_{\text{disk}}(R, z) = -\frac{GM_{\text{disk}}}{\sqrt{R^2 + [a_{\text{disk}} + (z^2 + b_{\text{disk}}^2)^{1/2}]^2}}, \quad (1)$$

where z is the vertical distance from the Galactic plane and R is the radial distance perpendicular to the Galactic central axis. This potential has an axisymmetric form ($q_a = 1$, $q_b = 1$). The parameters q_a and q_b determine the geometry of the disks, while a and b are scaling factors (Katsanikas et al. 2013). The spheroidal component of the Galactic gravitational potential is

$$\Phi_{\text{sph}}(R, z) = -\frac{GM_{\text{sph}}}{\sqrt{R^2 + [a_{\text{sph}} + (z^2 + b_{\text{sph}}^2)^{1/2}]^2}}. \quad (2)$$

The halo component is

$$\Phi_{\text{halo}} = \frac{GM_{\text{halo}}}{r_c} \left[\frac{1}{2} \ln \left(1 + \frac{R^2 + z^2}{r_c^2} \right) + \frac{r_c}{\sqrt{R^2 + z^2}} \arctan \left(\frac{\sqrt{R^2 + z^2}}{r_c} \right) \right], \quad (3)$$

where it is typically assumed that the value for the scale height of the Galactic halo, z , is 1.5 kpc . The numerical values of the parameters in the potential are summarized in Table 1.

The NSs are thought to be born mainly within the Galactic spiral arms, as these regions are rich in OB stars. There are several models for the pulsar number density n_{PSR} in our Galaxy. Following the approach by Schwarz & Seidel (2002), I assume that the NS number density n is not constant within our Galaxy but is proportional to n_{PSR}

$$n(R, z) = \frac{N_{\text{NS}}}{N_{\text{PSR}}} n_{\text{PSR}}(R, z), \quad (4)$$

where R is the Galactocentric distance of the pulsar/NS to the Galactic center in the Galactic plane and z is the scale height. In this work, I am mainly interested in the distribution of NSs as a function of distance from the Galactic plane, at a maximum Galactocentric distance of $R_{\text{max}} = 25 \text{ kpc}$.

The initial velocity in each NS is calculated as the vector sum of three different velocities: (1) a Maxwellian distribution, (2) a constant kick (non-Maxwellian), and (3) the

Table 2 Fraction of Bound Systems

	Halo (%)	Disk (%)	Mean Max 1-D velocity (km s ⁻¹)	1-D probability	3-D probability	<i>p</i> -value
Model <i>A</i>	43	43	413.1	0.43	0.78	0.09
Model <i>B</i>	41	45	315.6	0.45	0.79	0.091
Model <i>C</i>	51	53	299.2	0.53	0.83	0.0084

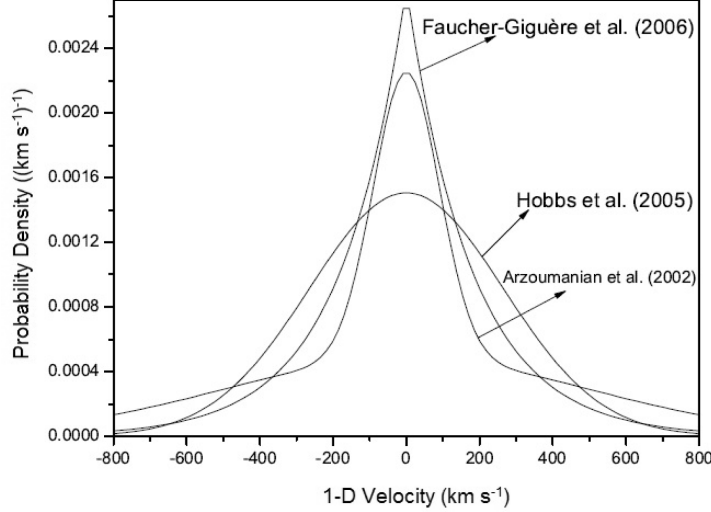


Fig. 1 The normalized 1-D velocity distributions of the three models: two Maxwellian components with velocity dispersions $\sigma_v \sim 90 \text{ km s}^{-1}$ (40% of the composition) and 500 km s^{-1} (60% of the composition) by Arzoumanian et al. (2002), a one-component Maxwellian distribution with velocity dispersion 265 km s^{-1} by Hobbs et al. (2005) and a one-component exponential distribution with a 3-D mean velocity of 380 km s^{-1} by Faucher-Giguère & Kaspi (2006).

circular rotation velocity at the birthplace (determined by Galactic gravitational potential). Here I choose the kick velocity v_k (Hansen & Phinney 1997) which is given by

$$P(v_k) = \sqrt{\frac{2}{\pi}} \frac{(v_k)^2}{\sigma_k^3} e^{-\frac{v_k^2}{2\sigma_k^2}}, \quad (5)$$

where σ_k is the dispersion of the velocity and recall that Hobbs et al. (2005) found $\sigma_k = 265 \text{ km s}^{-1}$. Fryer et al. (1999) and Cordes & Chernoff (1998) also proposed a bimodal distribution. I use velocity dispersion $\sigma_k = 190 \text{ km s}^{-1}$.

I consider three different initial kick distributions here: a bimodal distribution with two Maxwellian components; the velocity dispersion, σ , of the first peak is $\sigma_v \sim 190 \text{ km s}^{-1}$. The fraction of NSs in the first peak is about 40%. The second peak corresponds to $\sigma = 500 \text{ km s}^{-1}$ (Model *A*), having one Maxwellian component distribution with the 1-D velocity dispersion 265 km s^{-1} (Model *B*), and the other one is an exponential distribution with a 3-D mean velocity of 380 km s^{-1} (Model *C*). Every component of the kick velocity is randomly generated to have a random initial Maxwellian distribution according to the probability function (Eq. (4)). The normalized 1-D velocity distributions of the three models are presented in Figure 1.

The shape of the 3-D velocity distribution in different models is plotted in Figure 2.

3 SIMULATION RESULTS AND DISCUSSIONS

In Figure 1, I have plotted the normalized 1-D velocity probability density functions for the three models. All of them appear well defined and agree with the Gaussian distribution in terms of the mean. The widths were determined using robust statistics, with a standard deviation of 0.3 in most cases (the probabilities are reasonably accurate for our number of data points, see Press et al. 1992). The results are consistent with those obtained by Lorimer (2011). For the fractions of systems remaining bound for each of the kick distributions in each region around the same range, the *p*-values obtained with a 1-D Kolmogorov-Smirnov (K-S) significance test as well as the mean max in-Galactic-disk 1-D velocities for the three models are shown in Table 2. However, one can notice some differences between them. Model *C* is slightly steeper than Model *A* with less height in the tail while Model *B* is slightly broader than the other two models, and the tails have little weight in the K-S test. It appears that the most elongated shapes of models seem to better reproduce the real distribution. Thus, I conclude that models *A* and *C* are

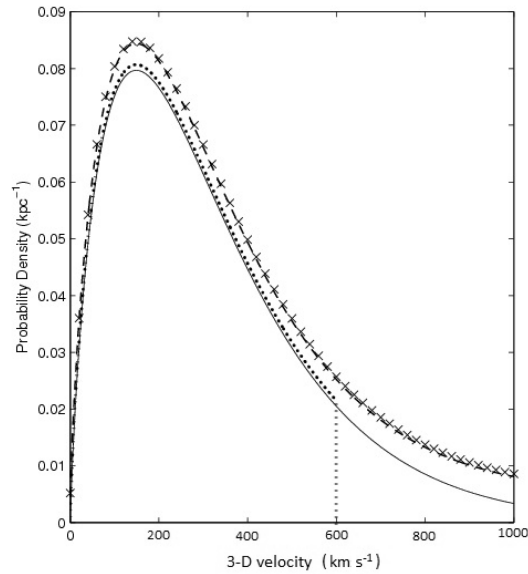


Fig. 2 The 3-D velocity distribution in the three models. The dotted line represents Hobbs et al. (2005). The cross line represents Faucher-Giguère & Kaspi (2006). The thin line represents Arzoumanian et al. (2002). All the distributions are normalized to unity.

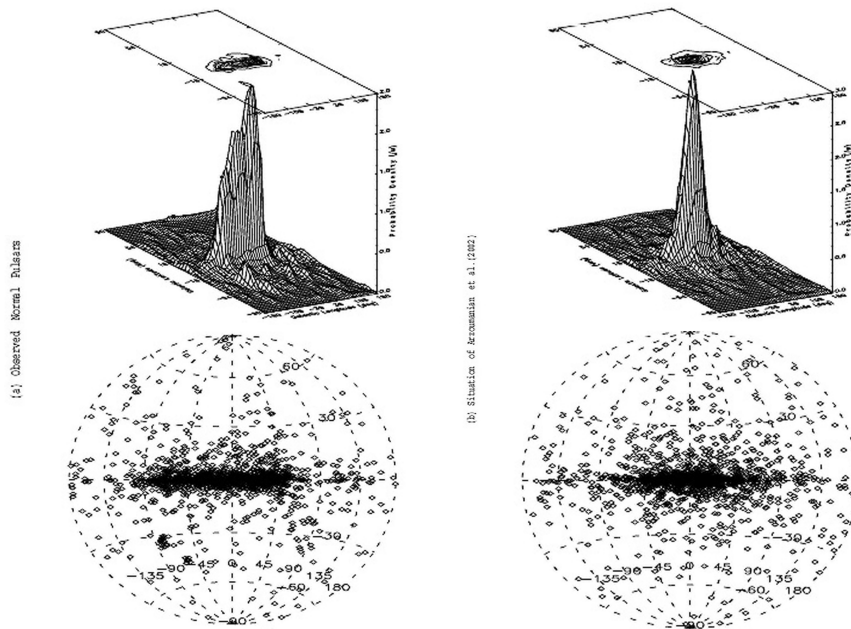


Fig. 3 The observed pulsars (the data are from the ATNF pulsar database, see Manchester et al. 2005) and the simulated old NSs $r \leq 25$ kpc, which were used in our analysis with initial velocity in Model A, are plotted in Hammer-Aitoff equal-area projection maps with Galactic coordinates (*lower*); their normalized probability density per unit solid angle with respect to the Galactic coordinates is also shown (*upper*).

favored compared to Model B and the NSs have a larger probability to get smaller initial kick velocities.

It is obvious that only if NSs have a small initial kick or possess a very low vertical velocity component (Tutukov & Bogomazov 2008) will they be likely to remain in the Galactic disk because they have a weak magnetic field. A detailed discussion on the effects of the NS magnetic

field is presented in Zhang & Kojima (2006) and references therein based on detailed evolutionary computations for a range of stellar models at different evolutionary stages. Because the z component of the velocity is strongly correlated with the total velocity, this approach could result in distortion in the derived velocity distribution. It is very interesting to notice that although Model A is similar to

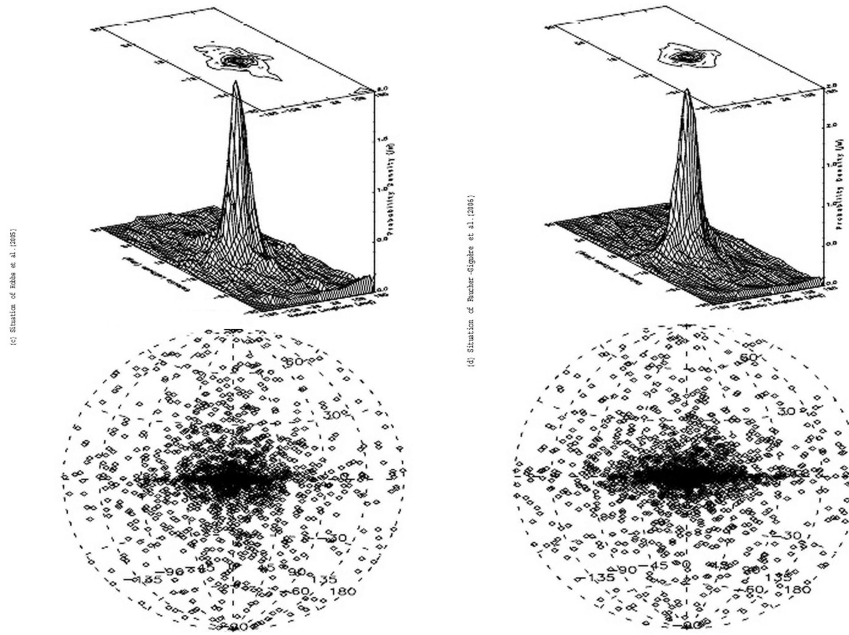


Fig. 4 The Hammer-Aitoff equal-area projection maps of Galactic coordinates (*lower*); their normalized probability density per unit solid angle with respect to Galactic coordinates (*upper*). The same as in Fig. 3 for Models *B* and *C* but with different initial conditions.

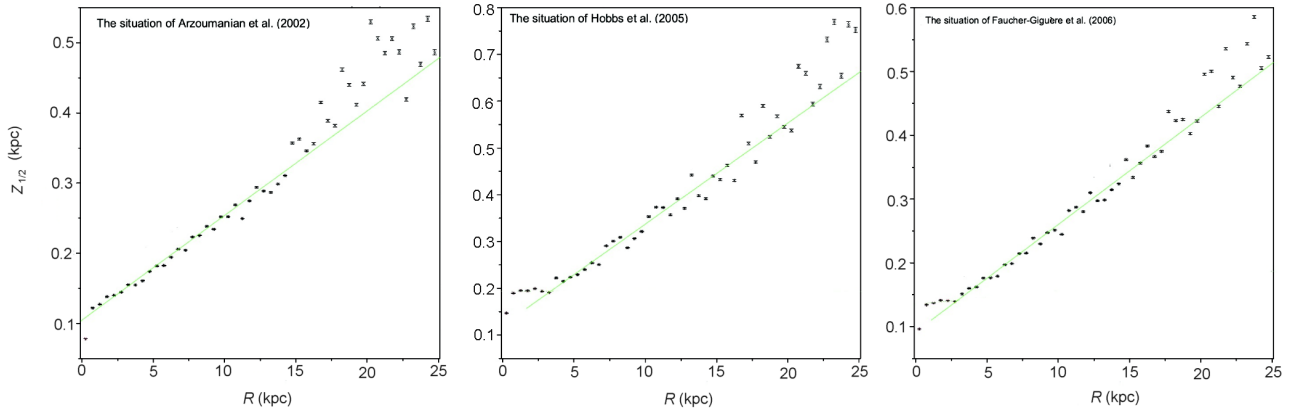


Fig. 5 A comparison of the scale-height variations of various distributions of simulated old NSs plotted as a function of the Galactocentric distance in Models *A*, *B* and *C*, from left to right respectively.

in-Galactic-disk as incorporated in Model *B*, the latter two refer to Models *B* and *C* having similar mean max in-Galactic-disk 1-D velocities. I should mention here that the typical rotation velocities of disk galaxies are in the range $100\text{--}300\text{ km s}^{-1}$ (Courteau et al. 2007). Schönrich (2012) finds $v_{\text{circ}} = 238 \pm 9\text{ km s}^{-1}$ for the solar neighborhood, at a distance $R \sim 8\text{ kpc}$ from the center of the Galaxy.

I have checked the consistency of the three models by comparing their velocity distributions with the K-S test. The K-S test demonstrates that the cumulative probability (P) and their 3-D distribution of NS velocities are growing with approximately the same rate as the remaining fraction in the Galactic disk with radius $r < 25\text{ kpc}$ (see Table 2). The statistics indicate a probability of 0.315 that the ve-

locities of the 1-D NSs are drawn from the same distribution. Comparison of the 3-D samples with the summed 1-D ones gives a similar value of 0.35. The p -value of the K-S test applied to the distribution is 0.09. The comparison may help us to further investigate the nature of the birth kick (Hartman 1997; Ng & Romani 2007) and also to establish evolutionary links between different classes of isolated NSs (see e.g. Popov et al. 2000; Manchester et al. 2005; Kaspi 2007; Haberl 2007; Rea & McLaughlin 2008; Popov et al. 2015 for recent reviews about the different subclasses).

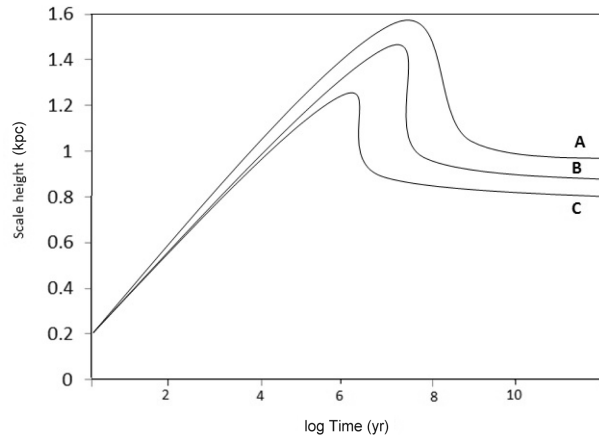


Fig. 6 The evolution track of scale height within Galactocentric distance from $R \sim 0 - 25$ kpc in different population models. Track *A* represents Arzoumanian et al. (2002). Track *B* represents Hobbs et al. (2005). Track *C* represents Faucher-Giguère & Kaspi (2006).

4 ANGLE DISTRIBUTION WITHIN THE GALACTIC DISK

Modeling the phase space of the distribution of old NSs may help us to gain insight into the advanced stages of dynamical evolution, in which compact objects are born from the supernovae deaths of their progenitors. The Galactic longitudes and latitudes of the observed pulsar distribution in the sky are graphically presented in Figure 3 (lower). This figure shows the distribution of observed pulsars on a Hammer-Aitoff equal-area projection in Galactic coordinates with the Galactic Center at the center of the plot. I plot the distribution of the simulated in-Galactic-disk NSs in Galactic coordinates (one point in the plot stands for 1000 NSs) and the distribution of observed normal pulsars ($P \geq 30$ ms) at Galactic latitudes $l \leq 5^\circ$. In addition, I also plot their normalized probability density per unit solid angle in space with the variables of Galactic longitudes and latitudes increasing to the left. Furthermore, the knowledge of this distribution is, therefore, fundamental to understanding the mechanisms involved in the final stages of spatial distribution and dynamical evolution as well as detection through the interstellar medium in X-ray observations.

In the comparisons between the simulated old NSs and the observed pulsars, I stress that both sample groups have different ages, implying an influence by the different evolutionary histories, since the age of observed normal pulsars is of order $\sim 10^7$ yr, while that of the simulated old NSs is of order $\sim 10^8$ yr. However, one should take into account various systematic errors caused by (1) the observational biases of the surveys owing to their luminosities, rotation periods, the orientations of the emission beam, the effect of the interstellar medium, as well as the ranges of surveys performed by radio telescopes, since the observed sample is a biased subset of the full Galactic pulsar population (Lorimer 2008); (2) instrumental selection effects (Lyne & Graham-Smith 2006); and (3) random and sys-

tematic errors caused by using a distance model (Gunn & Ostriker 1970).

The detected normal pulsars in our Galaxy are mainly clustered in the vicinity of the solar system (e.g. Kramer et al. 2003).

In Figure 3 (upper panel), it is clear that the distribution peak of normal pulsars is near the Galactic longitude 50° , and the lower panel from the same figure displays the distribution of Galactic coordinates for old NSs.

Figures 3 and 4 show the distributions of Galactic coordinates (lower) and their corresponding normalized probability density plots (upper). It can be noted that the probabilities of lying in the area with high Galactic latitude in Models *B* and *C* are larger than in Model *A*, since as the population gets older, due to the kick velocity at birth, they can move towards higher latitudes with timescales comparable to their characteristic ages and become more dynamic on the scale of the Galaxy. This is consistent with the large range of velocities for remaining-in-Galactic-disk NSs in Figure 1.

It is important to mention that our model parameters are chosen to give statistics about the distribution of the old NSs in the Galaxy, or derive a disk of the old NSs. In addition, I aim to investigate the qualitative relation between both structures at a radial velocity compatible with the kinematical distance in the old NSs. I plot the half density scale heights at different Galactocentric distances R in Figure 5, in order to facilitate the comparison between the three models. Furthermore, the scale height of the density distribution increases systematically with R between the three different models.

The half-density scale height of the global disk is $z_{1/2} = 0.176 \pm 0.00018$ kpc ($z_{1/2}$ is the height at which the probability density decays to 50% of the probability density at the Galactic plane $z = 0$). I also calculate the half-density scale height in the vicinity of the Sun with $z_{1/2} = 0.22 \pm 0.0004$, 0.22 ± 0.0004 and 0.23 ± 0.0003 kpc in the three different population models in Models *A*, *B*

and C respectively, suggesting that the half-density scale height is close to the vicinity of the Sun. I should mention here that the results of the half-density scale height in these models are quite close to the value calculated by P90 ($z_{1/2} = 0.193$ kpc). However, Hartmann et al. (1990) and Ofek (2009) found the values were $z_{1/2} = 0.5$ kpc and $z_{1/2} = 0.3 - 0.6$ kpc respectively. The difference is mainly due to different velocity distributions at birth and to different Galactic potentials. Finally, the evolution track of scale height within the Galactocentric distance of 0–25 kpc with different initial kick velocities that are adopted in different population models is plotted in Figure 6. A significant peak appears at different times during the evolution in each model. The shapes first increase linearly with the time period of $\tau \sim 10^{5-7}$ yr, reach the peak then gradually decrease, and finally approach a stable asymptotic value (constant value) at $\tau \sim 10^{7-9}$ yr, through the time evolution.

5 CONCLUSIONS

I have investigated the initial velocity and spatial distribution of the isolated old NS population in the Galaxy through a numerical simulation, by adopting three distributions of initial random velocity proposed by Arzoumanian et al. (2002), Hobbs et al. (2005) and Faucher-Giguère & Kaspi (2006) respectively. My aim with this paper was to study and compare different approaches towards the properties of the distribution of old NSs and their motion. I gave the NS scale heights at the different radial locations and their distributions in the Galaxy. Our simulation confirms the validity of the 3-D axisymmetric potentials and shows that the radial hierarchy and velocity effect can be regarded as the result of the dynamical evolution of the old NSs that originate from the Galactic disk. I clearly show the linear relationship of the cumulative scale height in three different models within the stellar disk radius at 0 – 25 kpc. Each segment has a linear relation with R , and the half-density scale height of the simulated NSs is approximately $z_{1/2} = 220 \pm 0.00018$ pc from the disk within the different models, which indicates that the disk thickness has a smaller characteristic size and different kinematics than in the Galactocentric distance.

The Hammer-Aitoff projection also shows that the conformal nature of the NS projections and simulation preserves shapes locally, which may be of particular use for analyzing their large scale structure. I have also shown that the simulated old NSs in these population models most likely share similar shapes in terms of 1-D and 3-D initial velocity distributions, as well as their evolution within the scale height. The probability distribution functions are consistent with those in the remaining fraction of NSs within Galactocentric radius $r \leq 25$ kpc due to the kicks obtained from different models. However, some kicks are more vulnerable, and some types of kicks are more effective than others; it is rare to see kicks that are more than 1000 km s^{-1} as in 2-D (Scheck et al. 2006) because it will require many more model runs that vary the initial random

seed perturbations as well as the stellar progenitor and explosion energy. In the future, many more observations of isolated old NSs will be achieved with the *eROSITA* all-sky survey (Merloni et al. 2012) of soft X-ray sources (0.5–2 keV).

Acknowledgements I specifically would like to acknowledge Ying-Chun Wei for his assistance with the simulation code. I would like to deeply thank Prof. Hamid Al-Naimiy, the chancellor of the University of Sharjah and the director of the Sharjah Center for Astronomy and Space Sciences, for his support. I also thank the anonymous referee for very helpful and constructive comments, which helped to improve the paper.

References

- Arzoumanian, Z., Chernoff, D. F., & Cordes, J. M. 2002, *ApJ*, 568, 289
- Binney, J., & Tremaine, S. 2008, *Galactic Dynamics: Second Edition* (Princeton Univ. Press)
- Brisken, W. F., Benson, J. M., Goss, W. M., & Thorsett, S. E. 2002, *ApJ*, 571, 906
- Chatterjee, S., & Cordes, J. M. 2004, *ApJ*, 600, L51
- Chierigato, M., Campana, S., Treves, A., et al. 2005, *A&A*, 444, 69
- Cordes, J. M., Romani, R. W., & Lundgren, S. C. 1993, *Nature*, 362, 133
- Cordes, J. M., & Chernoff, D. F. 1998, *ApJ*, 505, 315
- Courteau, S., Dutton, A. A., van den Bosch, F. C., et al. 2007, *ApJ*, 671, 203
- Dai, S., Smith, M. C., Lin, M. X., et al. 2015, *ApJ*, 802, 120
- Faucher-Giguère, C.-A., & Kaspi, V. M. 2006, *ApJ*, 643, 332
- Flynn, C., Sommer-Larsen, J., & Christensen, P. R. 1996, *MNRAS*, 281, 1027
- Fryer, C., Benz, W., Herant, M., et al. 1999, *ApJ*, 516, 892
- Gonthier, P. L., Story, S. A., Clow, B. D., et al. 2007, *Ap&SS*, 309, 245
- Gonthier, P. L., Story, S. A., Giacherio, B. M., et al. 2006, *ChJAA* (Chin. J. Astron. Astrophys.), 6s, 97
- Gunn, J. E., & Ostriker, J. P. 1970, *ApJ*, 160, 979
- Haberl, F. 2007, *Ap&SS*, 308, 181
- Han, Z. 2008, *ApJ*, 677, L109
- Hansen, B. M. S., & Phinney, E. S. 1997, *MNRAS*, 291, 569
- Hartman, J. W. 1997, *A&A*, 322, 127
- Hartmann, D., Woosley, S. E., & Epstein, R. I. 1990, *ApJ*, 348, 625
- Hobbs, G., Lyne, A. G., Kramer, M., et al. 2004, *MNRAS*, 353, 1311
- Hobbs, G., Lorimer, D. R., Lyne, A. G., et al. 2005, *MNRAS*, 360, 974
- Hu, T., Peng, Q.-H., & Zhao, Y.-H. 2006, *A&A*, 446, L5
- Janka, H.-T. 2012, *Annual Review of Nuclear and Particle Science*, 62, 407
- Kaspi, V. M. 2007, *Ap&SS*, 308, 1

- Katsanikas, M., Patsis, P. A., & Contopoulos, G. 2013, *International Journal of Bifurcation and Chaos*, 23, 1330005
- Kramer, M., Bell, J. F., Manchester, R. N., et al. 2003, *MNRAS*, 342, 1299
- Lai, D., Chernoff, D. F., & Cordes, J. M. 2001, *ApJ*, 549, 1111
- Lorimer, D. R. 2008, *Living Reviews in Relativity*, 11, arXiv:0811.0762
- Lorimer, D. R. 2011, *Astrophysics and Space Science Proceedings*, 21, 21
- Lyne, A. G., & Graham-Smith, F. 2006, *Pulsar Astronomy* (3rd edn., Cambridge: Cambridge Univ. Press)
- Manchester, R. N., Hobbs, G. B., Teoh, A., et al. 2005, *AJ*, 129, 1993
- Merloni, A., Predehl, P., Becker, W., et al. 2012, arXiv:1209.3114
- Miyamoto, M., & Nagai, R. 1975, *PASJ*, 27, 533
- Ng, C.-Y., & Romani, R. W. 2007, *ApJ*, 660, 1357
- Ofek, E. O. 2009, *PASP*, 121, 814
- Paczynski, B. 1990, *ApJ*, 348, 485
- Page, D., Lattimer, J. M., Prakash, M., et al. 2004, *ApJS*, 155, 623
- Plummer, H. C. 1911, *MNRAS*, 71, 460
- Podsiadlowski, P., Pfahl, E., & Rappaport, S. 2005, in *Astronomical Society of the Pacific Conference Series*, 328, *Binary Radio Pulsars*, eds. F. A. Rasio, & I. H. Stairs, 327
- Popov, S. B., Prokhorov, M. E., Colpi, M., et al. 2000, *astro-ph/0008199*
- Popov, S. B., Postnov, K. A., & Shakura, N. I. 2015, *MNRAS*, 447, 2817
- Press, W. H., Teukolsky, S. A., Vetterling, W. T., & Flannery, B. P. 1992, *Numerical Recipes in C. The Art of Scientific Computing* (Cambridge: Cambridge Univ. Press)
- Rea, N., & McLaughlin, M. 2008, in *American Institute of Physics Conference Series*, 968, *Astrophysics of Compact Objects*, eds. Y.-F. Yuan, X.-D. Li, & D. Lai, 151
- Scheck, L., Kifonidis, K., Janka, H.-T., et al. 2006, *A&A*, 457, 963
- Schönrich, R. 2012, *MNRAS*, 427, 274
- Schwarz, D. J., & Seidel, D. 2002, *A&A*, 388, 483
- Shklovskii, I. S. 1970, *Soviet Ast.*, 13, 562
- Spruit, H., & Phinney, E. S. 1998, *Nature*, 393, 139
- Sun, X. H., & Han, J. L. 2004, *MNRAS*, 350, 232
- Taani, A., Zhang, C. M., Al-Wardat, M., & Zhao, Y. H. 2012a, *Astronomische Nachrichten*, 333, 53
- Taani, A., Naso, L., Wei, Y., Zhang, C., & Zhao, Y. 2012b, *Ap&SS*, 341, 601
- Taylor, J. H., & Cordes, J. M. 1993, *ApJ*, 411, 674
- Tsuruta, S. 1998, *Phys. Rep.*, 292, 1
- Tutukov, A. V., & Bogomazov, A. I. 2008, *Astronomy Reports*, 52, 390
- Wang, B., & Han, Z. 2010, *Ap&SS*, 329, 293
- Wei, Y.-C., Wu, X.-J., Peng, Q.-H., Wang, N., & Zhang, J. 2005, *ChJAA (Chin. J. Astron. Astrophys.)*, 5, 610
- Wongwathanarat, A., Hammer, N. J., & Müller, E. 2010, *A&A*, 514, A48
- Wongwathanarat, A., Müller, E., & Janka, H.-T. 2015, *A&A*, 577, A48
- Wyrzykowski, Ł., Kostrzewa-Rutkowska, Z., Skowron, J., et al. 2016, *MNRAS* accepted, arXiv:1509.04899
- Yakovlev, D. G., & Pethick, C. J. 2004, *ARA&A*, 42, 169
- Zhang, C. M., & Kojima, Y. 2006, *MNRAS*, 366, 137
- Zhang, C. M., Wang, J., Zhao, Y. H., et al. 2011, *A&A*, 527, A83